MODELLING THE DEGRADATION BEHAVIOUR OF Z-PINS UNDER CYCLIC LOADING CONDITIONS

Felix Warzok[1], Giuliano Allegri[2], Maik Gude[3], Stephen Hallett[4]

[1]Advanced Composite Centre for Innovation and Science (ACCIS), University of Bristol, University Walk, Bristol BS81TR, United Kingdom
Email: felix.warzok@bris.ac.uk, Web Page: http://www.bristol.ac.uk/composites/
[2]Advanced Composite Centre for Innovation and Science (ACCIS), University of Bristol, University Walk, Bristol BS81TR, United Kingdom
Email: g.allegri@imperial.ac.uk, Web Page: http://www.bristol.ac.uk/composites/
[3]Institute of Lightweigth Engineering and Polymer Technology (ILK), Technische Universitaet Dresden, Holbeinstr. 3, 01307 Dresden, Germany
Email: maik.gude@tu-dresden.de, Web Page: http://www.tu-dresden.de/mw/ilk/
[4]Advanced Composite Centre for Innovation and Science (ACCIS), University of Bristol, University Walk, Bristol BS81TR, United Kingdom
Email: stephen.hallett@bris.ac.uk, Web Page: http://www.bristol.ac.uk/composites/

Keywords: CFRP, Z-pinning, Fatigue, Modelling,

Abstract
3D-reinforcements such as Z-pins can improve the delamination strength of composites substantially. They are thus of significant interest for safety critical thick composite structures. For structural applications the effect of fatigue on these 3D-reinforcements needs to be investigated to assess the behaviour of a Z-pinned component after being in service for a while or after a major impact event has taken place. Here the findings from a previous micro mechanical study characterising the behaviour of Z-pins under various fatigue loading conditions are transferred into an analytical/numerical model and validated with bespoke meso scale DCB and ELS tests. Good agreement between simulation and experiment was found for most load cases, however, the model seems slightly to overpredict the degradation in mode I loading scenarios for small amplitudes and medium average pin displacements.

1. Introduction

Z-pinning has proved to be an effective technology for enhancing the through-thickness (TT) properties of Prepreg laminates [1]. It utilises small high stiffness and/or high strength rods, which are inserted into a laminate before curing. However, much of the research on Z-pinned composites is limited to quasi-static loading and less is known about the behaviour under in-service conditions, which is likely to include vibration and repeated loading.

In a micro-mechanical study, Zhang et al. [2] performed cyclic mode I tests on specimens reinforced with a Z-pin array. An ongoing decrease of the static peak load P was found in residual tests when fatiguing the specimens before reaching P. Even though, further pull-out did not show an obvious decrease of the frictional loads. A continuous decrease of the cyclic peak load was recorded during the fatiguing.

Pegorin et al. [3] showed the positive effects of Z-pins during fatigue in an experimental study on

Excerpt from ISBN 978-3-00-053387-7

the fatigue properties of pinned DCB and ENF coupons. In order to assess the fatigue strength, the amplitude $\Delta\delta$ and thus the interlaminar strain energy release rate G was increased during testing. The effectiveness of the through-thickness reinforcement (TTR) was assessed by monitoring the crack growth speed. Increasing the Z-pin density raised the fatigue delamination onset stress, as well as the critical G that corresponded to unstable crack propagation. At the same time, delamination propagated at a slower rate. Pins were more effective in mode I than in mode II. No effect of the applied amplitude could be discerned.

Due to the small embedded pin length of 3 *mm* in both these studies the understanding of the effect of important fatigue parameters like average displacement δ_0, amplitude $\Delta\delta$ is limited.

A comprehensive experimental characterisation of the mechanical property degradation of individual Z-pins and the laminate/pin interface under cyclic loading conditions through testing of single pin specimens has been undertaken by Warzok et al ([4]). Different fatigue test setups were investigated altering:

- Fracture mode (I & II)
- Mean displacement during fatigue δ_0
- Amplitude $\Delta\delta$
- Number of cycles n

For mode I a continuous degradation of energy dissipation was found during fatigue cycling and in residual testing (Fig. 1). The main influence on the degradation was the applied $\Delta\delta$ and, to a lesser extent, δ_0 and n. A phenomenological model for describing the degradation of fatigue and residual properties was presented. For mode II testing no significant change of residual properties could be found below a critical upper displacement $\delta_u = \delta_0 + \Delta\delta$, that lead to pin rupture within a limited number of cycles. The small degradation of residual energy dissipation measured can be attributed to the softening of the surrounding resin pocket and thus lower load bearing in the previously fatigued section when restarting the test (Fig. 1b).

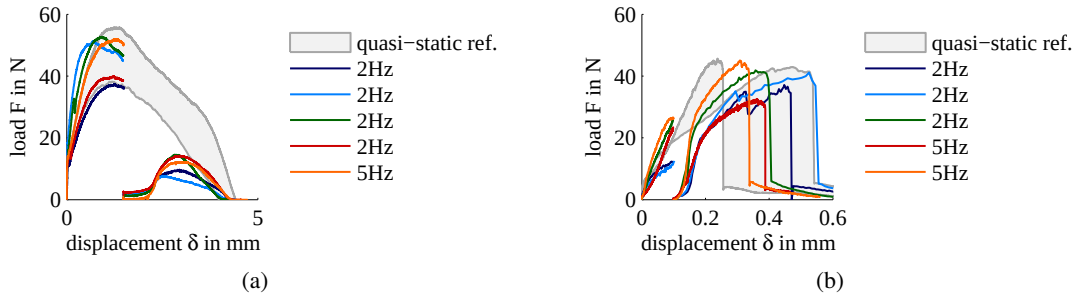

Figure 1: Single Pin pre- and post-fatigue results from [4] for (a) mode I ($\delta_0 = 1.5\ mm$, $\Delta = 0.8\ mm$, $n = 10^5$) and(b) mode II ($\delta_0 = 0.1\ mm$, $\Delta = 0.05\ mm$, $n = 10^5$).

In this study the findings of [4] are transferred into a combined numerical/analytical model in which the quasi-static specimen performance is modelled numerically while the fatigue degradation is calculated analytically. A novel experimental setup is presented to validate the results.

Excerpt from ISBN 978-3-00-053387-7

2. Specimen manufacture

Modified DCB and ELS specimens are used for validation purposes (Fig. 2). The distribution of pin rows along the specimen length ensures, that each of these rows experiences slightly different fatigue mean displacements and amplitudes. Specimen dimensions are 155 mm x 20 mm x 8 mm. The specimen length has been chosen to allow for an even pin distribution with a large enough distance between the pins to allow for varying fatigue parameters and a small enough distance to prevent sudden crack growth. Z-pin insertion leads to small changes of the in-plane fibre architecture. The chosen specimen width prevents the accumulation of fibre deviations along the pin rows. Since the embedded pin length has a significant effect on pin performance, the specimen thickness has been kept consistent with [4] at 8 mm. An FEP flouropolymer film was inserted in the mid plane to exclude the effect of delamination crack growth at the ply interface under fatigue and facilitate the measurement of pin loads only. For the same reason the specimens were clamped at 130 mm in the length-direction to prevent early sudden crack growth. The end of the ELS-specimen is free to move horizontally to avoid the introduction of additional tensile loads.

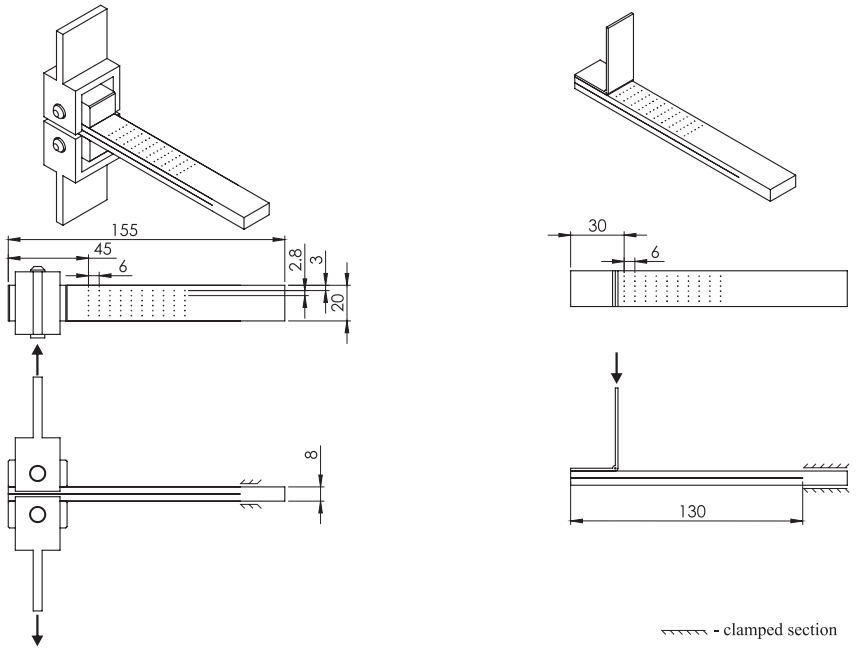

Figure 2: Sketches of (a) DCB and (b) ELS specimens. A 130 mm pre-crack is introduced.

A zero-dominated 64-ply layup (stacking sequence: $[(45/0/-45/0)_{4s}/*/(-45/0/45/0)_{4s}]$) is used. The $\varnothing = 0.28\ mm$ carbon pins are inserted manually, as described in [4], to reduce pin misalignment.

In the DCB specimens the load is applied during testing via bolted blocks and a clevis. To prevent instabilities during fatigue testing the bolts and holes were manufactured with a H7/g6 tolerance. Using metallic hinges was not possible for these specimens due to the disadvantageous loading conditions on the glue and the high loads caused by the pins and the stiff composite material. In contrast, metallic hinges could be utilised for the ELS specimens. These were oriented in such way that the stiffened part of the ELS does not affect the load measurements. Both, hinges and blocks are fixed to the specimen using Araldite 2014 epoxy glue. A grey scale pattern is applied to the specimens for accurate deformation measurements using optical techniques.

Excerpt from ISBN 978-3-00-053387-7

3. Experimental Procedure

An overview of the test configurations is given in table 1. The specimens are deformed initially up to δ_0. Subsequently $\Delta\delta$ is applied for a given number of cycles, n. Finally the quasi-static test is continued to capture the residual properties. For the DCB specimens two setups with small δ_0 and $\Delta\delta$ are chosen, to represent vibrating thick composite structures in the presence of significant, but possibly undetected cracks. The third configuration with large deformations is chosen for model validation purposes mostly. These are noted as fatigue regimes 1 to 3 ($F1$ etc.) The two fatigue configurations chosen for ELS testing cover nearly the whole range of applicable displacements during fatigue before pin rupture and are thus well suited for validation purposes. In [4] no effect of n could be determined, which will be trialled by cycling with the same parameters for 10^5 and $5 * 10^5$ cycles. Fairly large displacements are applied, which could represent an intact but damaged safety-relevant structure after a major impact event. The numerically obtained pin displacements within the applied fatigue test series are given in Fig 3. 3 reference pure quasi-static tests have been performed for each fracture mode

Table 1: Experiment matrix.

	$\delta_0(mm)$	$\Delta\delta(mm)$	n	number of tests
DCB_{F1}	0.7	0.2	10^5	3
DCB_{F2}	3.25	0.2	10^5	3
DCB_{F3}	8.2	1.5	10^5	5
ELS_{F1}	4.1	1.36	10^5	3
ELS_{F2}	4.1	1.36	$5 * 10^5$	3

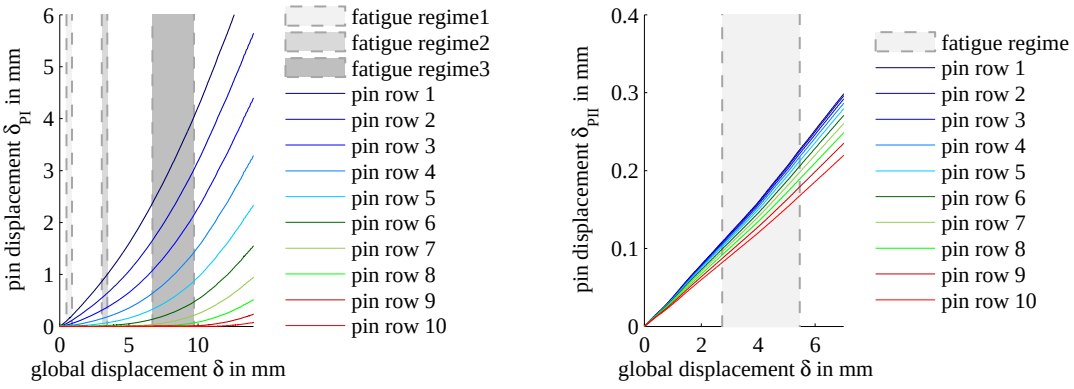

Figure 3: Pin displacements for the chosen fatigue loading regimes in (a) DCB and (b) ELS specimens.

For both the mode I and mode II tests, the measured load is made up of the pin response and the specimen compliance. Since the compliance is relatively high in the ELS-tests, the quasi-static deformation of these is repeated after all pins have failed to separately measure the compliance related response. The quasi-static tests and limited periods of the fatigue tests are recorded with a video camera (0.2 frames per second, 1920x1080 resolution) and analysed with Aramis® software.

Excerpt from ISBN 978-3-00-053387-7

4. Simulation

4.1. Numerical

The numerical analysis is run in the explicit finite element software package LS-Dyna. A sketch of the DCB model is given in figure 4. For the ELS model this is basically the same without modelling the load application blocks explicitly. Each pin is represented individually using one cohesive element with an edge length of 0.248 mm. The crucial cohesive material constants, taken from [4] and normalised by pin area, are given in Table 2. The chosen pin material model allows the definition of a normalised traction-separation curve, which is computed in such way that the curve peak matches the provided strengths σ_I/σ_{II} and the area under the curve corresponds to the entered critical energy release rate G_c. Strength, energy and traction-separation curve were taken from the micro scale experiments carried out in [4]. However, for mode II these had to be reduced by approximately 10% to account for the more pure mode II conditions in an ELS test than the near mode II tests in [4] (specimens were offset by 3 to avoid interface fraction). For the release film low values have been chosen arbitrarily for σ_I, σ_{II} and G_c to prevent any significant effect on the output response. Standard steel properties have been assumed for the load application blocks in the DCB tests. The composite material input has been derived from the UD material constants provided by Hexcel [5]. A comparison of numerically and experimentally determined traction-separation curves for mode I and II is given in Fig. 5.

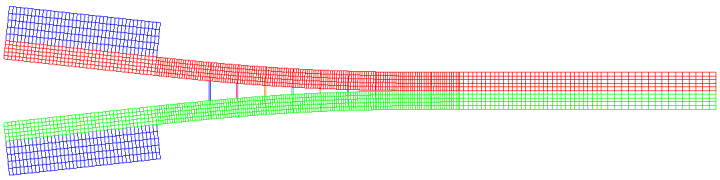

Figure 4: Numerical DCB model midway through analysis.

Table 2: Cohesive material properties.

	G_{IC} $[J/m^2]$	G_{IIC} $[J/m^2]$	σ_I $[MPa]$	σ_{II} $[MPa]$
Pin	1950.0	144.0	682.0	661.0
Release Film	1.0E-6	1.0E-6	1.0E-3	1.0E-3

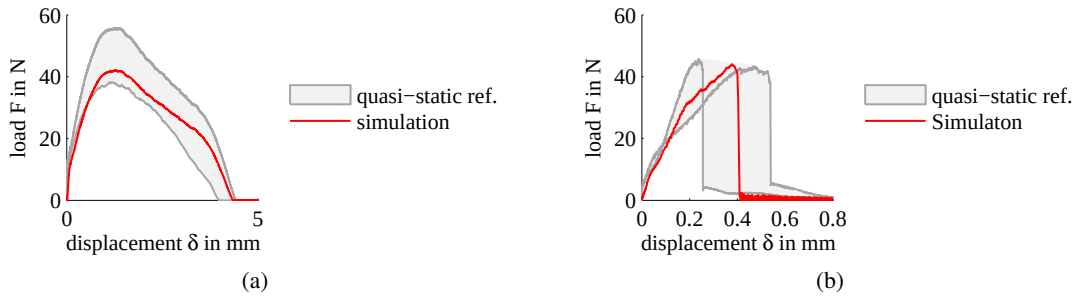

Figure 5: Numerically and experimentally determined single pin curves for (a) mode I and (b) mode II.

Excerpt from ISBN 978-3-00-053387-7

4.2. Analytical

Two runs of the finite element analysis are needed for obtaining the post-fatigue specimen performance. A first run is performed to calculate the pin displacements as a function of global displacement. This information is then read by a Matlab script in which the user can specify the desired fatigue parameters δ_0, $\Delta\delta$ and n. The Matlab script then calculates the corresponding pin displacements of each pin row and, based on these, the reduction in G due to the fatigue loading. Thus, each row of pins needs an individual material model. For mode I the degradation is calculated using the model proposed in [4]. For the mode II post-fatigue properties it was not possible to derive an analytical model for the reduction in G from the single pin data [4]. However, it was shown that the energy loss was mostly caused by the load reramping up from values close to 0 after the fatigue, instead of maintaining the expected load levels. Accordingly, the Matlab script reduces the nominal load traction-separation curve used to define the cohesive material model to 0.01 when reaching δ_0. The expected nominal load is recovered when the maximum pin displacement during fatigue δ_u is reached. The total cohesive energy is reduced accordingly.

5. Results and Discussion

Fig. 6a shows the experimental results of the quasi-static reference DCB-tests. A steep load increase can be observed while the number of pins bridging the crack increases. Once the first pins start pulling out, a slow load decrease starts, which accelerates towards the end of the test. Sudden crack growth until the clamped section of the DCB has been observed in some tests. In comparison to single pin tests, where pins always pulled-out completely, small portions of pin rupture have been observed during the quasi-static loading in all test series. Additionally, some pins ruptured in fatigue, especially for the fatigue configuration with large specimen opening, leading to high scatter on the post-fatigue results. This was not reported previously and is attributed to the slightly higher mixed mode ratios in the DCB-tests, caused by cantilever bending and high pull-out displacements of the Z-pins, compared to the single pin tests carried out in [4]. No pin rupture was reported in [3]. However, a significantly lower embedded pin length and a different laminate layup were used compared to the current study. Due to the smaller forces acting on a pin in a thinner laminate, a lower embedded pin length could allow for a more robust pin design. The DCB fatigue results confirm the experimental finding in [4]. While very small values of $\Delta\delta$ cause no significant degradation in the residual response, notably lower load levels are reached after restarting the quasi-static test for DCB_{F3}, which has much greater δ_0 and $\Delta\delta$.

Fig. 6a also shows a the numerically obtained DCB results. The model curve aligns very well with the tests and captures both the load increase and decrease very well. Extending the LS-Dyna simulation with the described fatigue model leads to the curves shown in Fig. 6b- 6d. While the numerically obtained curves for fatigue configurations DCB_{F1} and DCB_{F3} show good agreement with the experimental results, the model over predicts the degradation for DCB_{F2} slightly, caused by an overestimation of the δ_0 influence on the degradation.

Results for the quasi-static ELS tests are shown in Fig. 7a and 7b. A gradual failure of the Z-pin rows occurs at around 8 mm displacement. The further load increase is caused by the compliance of the specimen only. For a better illustration of the pin loads the output response is reduced by the compliance in Fig. 7c and 7d. As described in [4] the fatiguing does not lead to a significant change to the output response - independently from the number of applied cycles. The overall curve shape looks very close to the ones reported for single pin tests. In comparison to the quasi-static tests the fatiguing seems to cause a more even strength level between the pin rows, leading to a sudden instead of a gradual failure. Again, the numerically obtained curve is well aligned with the experiments and captures compliance, pin loads and pin rupture very well. The same is true for the fatigue results. The effect of more sudden failure is

Excerpt from ISBN 978-3-00-053387-7

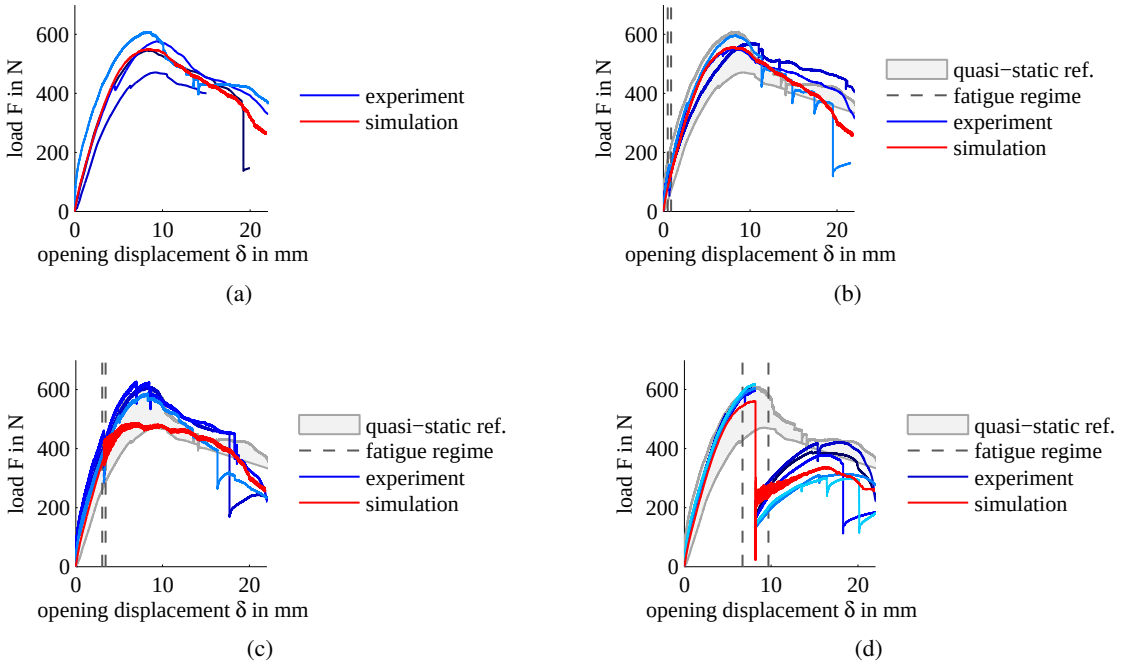

Figure 6: Experimental and numerical DCB results for (a) quasi-static reference (b) DCB_{F1}, (c) DCB_{F2}, (d) DCB_{F3}.

not captured, though.

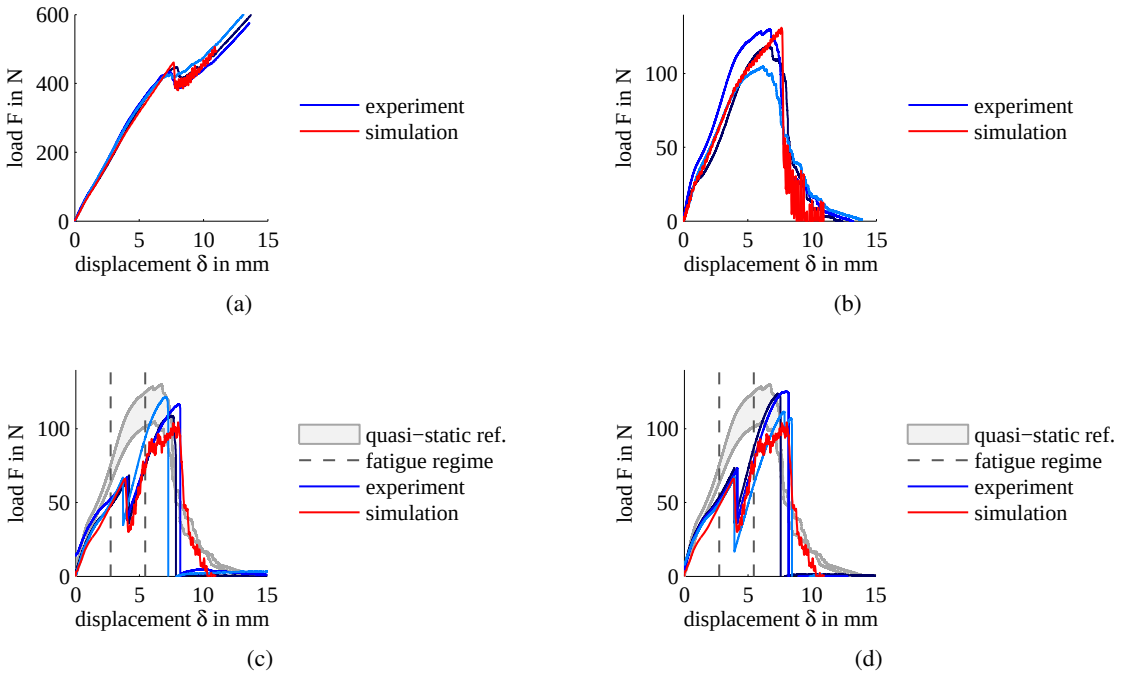

Figure 7: Experimental and numerical ELS results for quasi-static reference ((a) total load output and (b) reduced by compliance), (c) ELS_{F1} and (d) ELS_{F2}.

Excerpt from ISBN 978-3-00-053387-7

6. Conclusion

A numerical model for Z-pins has been extended by an analytical description of their fatigue degradation behaviour. The analytical solution was derived from the experimental findings in [4]. Modified DCB and ELS specimens have been used for validation purposes. These were artificially pre-cracked with an FEP release film at the mid plane so that the specimen load response comprised only the specimen compliance and the 3D-reinforcement. No fatigue effect of the matrix at the central ply interface was thus included in the model nor measured in the experimental tests.

The experiments verified the micro-scale findings reported in [4]. However, small portions of pin rupture occurred in the DCB tests both during the quasi-static and the fatigue experiments. Very good correlation for small and large fatigue displacements was found for the experimental and numerical results in mode I and II. The fatigue degradation was overestimated for small $\Delta\delta$ and medium δ_0, though. Due to the fatigue degradation of the 3D-reinforcements the length of bridging zone in the specimens increase slightly during the fatigue tests. However, this effect was insignificant for the trialled number of cycles and has not been considered.

Future work will focus on high cycle fatigue for mode I. Moreover, the analytical degradation model will revised to give a better correlation for mode I tests. This could be done by applying different weights to the influence of δ_0 and $\Delta\delta$. Finally, the adjustment of the mode II cohesive properties in the numerical simulation will be verified by another test series.

Acknowledgments

The authors would like to acknowledge Rolls-Royce Plc and the EPSRC for their support of this research through the Composites University Technology Centre (UTC) at the University of Bristol and grant no. EP/L505365/1 respectively.

References

[1] A.P. Mouritz. Review of z-pinned composite laminates. *Composites Part A: Applied Science and Manufacturing*, 38:2383–2379, July 19-24 2007.

[2] A.-Y. Zhang, H.-Y. Liu, A.P. Mouritz, and Y.-W. Mai. Experimental study and computer simulation on degradation of z-pin reinforcement under cycle fatigue. *Composites Part A: Applied Science and Manufacturing*, 39:406–414, 2008.

[3] F. Pegorin, K. Pingkarawat, and A.P. Mouritz. Comparative study of the mode i and mode ii delamination fatigue properties of z-pinned aircraft composites. *Materials and Design*, 65:139–146, 2015.

[4] F. Warzok, G. Allegri, M. Gude, and S.R Hallett. Experimental characterisation of fatigue damage in single z-pins. *Composites Part A: Applied Science and Manufacturing*, 2016.

[5] Hexply 8552 data sheet. Accessed: 2016-03-23.

Excerpt from ISBN 978-3-00-053387-7